Korean J. Chem. Eng., 35(7), 1532-1541 (2018)
DOI: 10.1007/s11814-018-0062-4

pISSN: 0256-1115
eISSN: 1975-7220

Immobilized titanium dioxide/powdered activated carbon system for the photocatalytic adsorptive removal of phenol

Noor Nazihah Bahrudin† and Mohd Asri Nawi

School of Chemical Sciences, Universiti Sains Malaysia, 11800 Penang, Malaysia
(*Received 12 December 2017 • accepted 5 April 2018*)

Abstract−Titanium dioxide (TiO_2) and powdered activated carbon (PAC) were fabricated via a layer by layer arrangement on a glass plate using a dip-coating technique for the photocatalytic-adsorptive removal of phenol. Thinner TiO_2 layer coated on PAC sub-layer has larger surface area and better phenol removal than the thicker TiO_2 layer. The system obeyed the Langmuir isotherm model, which exhibited a homogeneous and monolayer adsorption with a maximum capacity of 27.8 mg g^{-1}. The intra-particle diffusion was the rate-limiting step as the linear plot crossed the origin, while the adsorption was unfavorable at elevated temperature. Under light irradiation, the TiO_2/PAC system removed phenol two-times more effectively than the TiO_2 monolayer due to the synergistic effect of photocatalysis by TiO_2 top layer and adsorption by PAC sub-layer. The COD removal of phenol was rapid for 10 mg L^{-1} of concentration and under solar light irradiation. It was shown that the PAC sub-layer plays a significant role in the total removal of phenol by providing the adsorption sites and slowing down the recombination rate of charge carriers to improve the TiO_2 photocatalytic oxidation performance.

Keywords: Layer by Layer, Monolayer Adsorption, Photocatalytic Oxidation, Powdered Activated Carbon, Synergistic Effect

INTRODUCTION

New chemical compounds, mostly phenol-based structure, are synthesized frequently to fill industrial demand [1]. Having a benzene ring and a hydroxyl ion, phenol is the main substance used in plastic industry, agriculture, hospitality and cosmetic; thus significant amounts may be found in the corresponding wastewaters. Phenol is largely synthesized (<95%) by the cumene process (alkylation of benzene with propene) or toluene-benzoic acid process [2]. In addition, phenol is also one of the common intermediate products of the oxidation of higher molecular aromatic and phenolic compounds [3]. The toxicity of phenol is due to its benzene ring, which strongly inhibits biological degradation by common methods, the formation of free radicals and possibility of respiratory cancer and heart disease [4]. Phenolic compounds can change the taste and odor in the chlorinated water; therefore, a fixed low admissible level of 0.5 mg L^{-1} of the waterbody is permitted [5]. Hence, it is urgent to find the best way to treat this problematic organic material before releasing it into the mainstream.

The removal of water pollutants such as phenol by adsorption process may be the best method in water treatment due to the availability of many types of adsorbent [6]. The experimental conditions and parameters in adsorption studies can be used to provide some insights in determination of various mechanisms and interactions underlying the adsorption process [7]. However, one problem associated with adsorption is that it is an accumulation process which simply removes the pollutants from the effluent from one phase to another phase, i.e., from the liquid phase to solid phase without destroying them completely [4,8]. Nowadays, photocatalysis is considered among the most popular methods in wastewater treatment research as the process can convert the pollutants in the form of environmentally compounds such as CO_2 and H_2O [9]. As one of the advanced oxidation processes (AOPs), photocatalysis can produce powerful hydroxyl radicals ($^{\bullet}OH$) in the presence of H_2O and O_2 initiated by light energy that can surpass the photocatalyst's band gap energy. The radicals are attained when the H_2O and O_2 react with the positive hole at the valence band and the excited electron at the conduction band of the photocatalyst, respectively via the redox reaction, which will then destroy the organic pollutants to CO_2 and H_2O [9]. A successful photocatalysis process is indicated by the degree of mineralization of the pollutants which is usually measured based on the amount of carbonaceous substances in the treated water using indicators such as chemical oxygen demand (COD) and total organic carbon (TOC) analyses [10,11].

The adsorption and photocatalysis processes are usually combined to obtain a system with high synergistic effect to remove the pollutants [12,13]. In this case, powdered activated carbon (PAC) and titanium dioxide (TiO_2) are the suitable materials to carry out the task. PAC is a universal adsorbent and has a well-known reputation to adsorb phenolic compounds [14], while TiO_2 is the preferable photocatalyst due to its being photostable, biologically and chemically inert and inexpensive [15]. TiO_2 and PAC have been made as composites [16-18], mostly to enhance the adsorption capacity of TiO_2 since the photocatalytic oxidation process occurs on the photocatalyst's surface [19] and are applied in suspended or

†To whom correspondence should be addressed.
E-mail: nazihah.noor@yahoo.com

immobilized mode. However, the immobilized mode is more suitable for a real application since the fabricated system on support materials can be reused, needs no tedious filtration as well as potentially shows similar photoactivity as in suspended mode [20]. In addition, the easy operation economically reduces the overall cost of water treatment. The binding or immobilization process of TiO_2 and PAC on supporting materials is varied, depending on the experimental scale, cost and equipment used. For example, Shi et al. immobilized TiO_2 film on PAC by sol-gel adsorption [21], while Puma et al. prepared TiO_2 loaded AC support by chemical vapor deposition (CVD) [22]. Others used spray pyrolysis deposition [23,24], direct current magnetic sputtering [25], strewing method [15] and atomic layer deposition [26] in the fabrication of the photocatalyst on the suitable supports.

Our interest was to fabricate TiO_2 and PAC as an immobilized layer by layer assemblage via the cheap and convenience dip-coating method on the glass plate to remove phenol. In this arrangement, TiO_2 is the top layer while PAC is the adsorbent sub-layer. Although a similar type of assemblage system was reported previously by our groups using chitosan [20] and montmorillonite [19], we believe that this study is the first work on immobilized PAC as the adsorbent sub-layer of TiO_2 for the photocatalytic-adsorptive removal of phenol. The preliminary study on the suitability of PAC as the sub-layer for TiO_2 and the advantages of this layer by layer system have been discussed in the published article [27]. In the present manuscript, we extensively studied the adsorption characteristics of this layered system using adsorption modelling, while the mechanism of phenol adsorption was also proposed. The surface morphology, cross-section and optical property of the systems were analyzed using scanning electron microscopy (SEM) and photoluminescence (PL), respectively. The photocatalytic-adsorptive removal efficiency, reusability and COD removal by TiO_2/PAC system were then observed under an indoor lamp and solar light irradiation against the TiO_2 monolayer.

EXPERIMENTAL

1. Materials

Titanium (IV) oxide (TiO_2; CAS No: 13463-67-7) was purchased from Jebsen & Jessen Chemicals (M) Sdn. Bhd., while powdered activated carbon (PAC) was obtained from a local manufacturer. PAC was pre-treated with 1.0 M hydrochloric acid (HCl; 37% fuming; CAS No: 7647-01-0; Merck) for overnight, washed with enough distilled water to remove metal impurities and dried in the oven for 24 h at 110 °C. The polymer, poly (vinyl) chloride (PVC; CAS No: 9002-86-2) in white powder form was obtained from Petrochemicals Sdn Bhd whereas, epoxidized natural rubber with 50% mole of epoxidation (ENR_{50}) was from Guthrie Group (M) Sdn. Bhd. Toluene (C_7H_8; CAS No: 108-88-3) and dichloromethane (CH_2Cl_2; CAS No: 75-09-2) for dissolving ENR_{50} and PVC powder, respectively, were purchased from R&M Chemicals, while methanol (CH_3OH; CAS No: 67-56-1; HPLC grade) was bought from Merck. The model pollutant, phenol (C_6H_5OH, 99.5%; CAS No: 108-95-2), procured from Scharlau was diluted to appropriate concentrations for further use. Ultra-pure water (18 MΩ-cm) was used for all solution preparation. The phenol solution was kept at ambient pH (6.0).

2. Preparation of TiO_2/PAC

This layer by layer assemblage system was designed to remove phenol via concurrent dual processes of adsorption by the PAC sub-layer and photocatalytic oxidation by the TiO_2 top layer upon light irradiation. Therefore, the TiO_2 and PAC formulations were prepared in a separate bottle, respectively. The TiO_2 formulation was prepared according to the published method [28]. Briefly, 6 g of TiO_2 powder was added to a mixture of ENR_{50}/PVC adhesive blend and was sonicated for 8 h to obtain a homogenized milky white dispersion. The PAC formulation was prepared accordingly, but the amount of PAC used was 10 g [27]. For immobilization, glass plates with dimensions of 7.0 cm×4.7 cm and 0.2 cm thickness were selected. They were cleaned, rinsed with distilled water and technical grade acetone, air-dried and were weighed individually. Using different custom-made coating cell, the glass plate was first dip-coated in PAC formulation as the adsorbent sub-layer. Between each dipping, the coated plate was dried using a hair dryer to evaporate the toluene-dichloromethane solvent. The coated layer at the back, bottom and both sides of the plate was scraped off before weighing and leaving only the front layer [19,28]. These processes of dipping and drying the coated plate were repeated until the desired weight of 2.5 mg cm^{-2} of immobilized PAC was achieved. Similar procedures were followed for the coating of TiO_2 of desired weights as the upper layer. Such a layer by layer system was hereafter called as immobilized TiO_2/PAC.

3. Physical Characterizations

The surface morphology of TiO_2 layer of different loadings and the cross-section of TiO_2/PAC were observed via a scanning electron microscopy (model LEO SUPRA 50 VP Field Emission). The surface area, pore diameter and pore volume were obtained using a surface analyzer (Nova Quantachrome 2000). The samples were immobilized on the glass plates based on the required loadings and scrapped off from the plate for the analysis. The photoluminescence (PL) analysis for immobilized TiO_2, PAC and TiO_2/PAC was done by PL spectroscopy (HR800 UV) from Joblin Yvon at the excitation wavelength of 325 nm and was recorded at 300-1,000 nm scan range.

4. Statistical Analysis

The adsorption data at equilibrium was fitted into the non-linear form of isotherm models by "trial and error" approach using *Solver* function add-in Microsoft Excel. The amount of phenol adsorbed on TiO_2/PAC at equilibrium, q_e (mg g^{-1}) and the removal efficiency (R) were calculated as follows:

$$q_e = \frac{(C_o - C_e)V}{W} \quad (1)$$

$$R\,(\%) = \frac{(C_o - C_e)}{C_e} \times 100 \quad (2)$$

Here, C_o is the initial phenol concentration (mg L^{-1}), C_e is the concentration of phenol at equilibrium (mg L^{-1}), V is the volume of phenol solution (L) and W is the dry mass of TiO_2/PAC (g). The coefficient of determination (R^2), Chi-square (χ^2) test and residual-root-mean-square (RMSE) were used to determine the most fitted criteria of the adsorption isotherm model and the closeness of agreement between the experimental values of the amount of

phenol adsorbed at equilibrium ($q_{e,exp}$) with the calculated amount of phenol adsorbed at equilibrium from the model ($q_{e,cal}$) [29]:

$$R^2 = 1 - \frac{\Sigma_{n=1}^{n}(q_{e,exp.n} - q_{e,cal.n})^2}{\Sigma_{n=1}^{n}(q_{e,exp.n} - \overline{q_{e,exp.n}})^2} \quad (3)$$

$$\chi^2 = \sum_{n=1}^{n} \frac{(q_{e,exp.n} - q_{e,cal.n})^2}{q_{e,exp.n}} \quad (4)$$

$$RMSE = \sqrt{\frac{1}{n-1}\sum_{n=1}^{n}(q_{e,exp.n} - q_{e,cal.n})^2} \quad (5)$$

5. Adsorption and Photocatalytic-adsorptive Removal Studies

The adsorption studies were carried out using 20 mL of 10 mg L^{-1} phenol unless was stated otherwise. The experiment was conducted at several variables such as TiO_2 loadings (0.0-3.2 mg cm^{-2}), initial concentrations (10-100 mg L^{-1}) and reaction temperature (30-60 °C) within 90 min of contact time. The coated TiO_2/PAC plate was put vertically in a custom-made glass cell (8.0 cm×5.5 cm×1.0 cm) containing phenol solution and was sealed with a box to prevent light interference. Aeration was supplied from an aquarium pump through a Pasteur pipette dipped in the cell connected by PVC tubing and the rate was measured by a Gilmont flow meter. Meanwhile, the photocatalytic oxidation experiment was done under the irradiation of a 45-W compact home fluorescent lamp of 6.0 Wm^{-2} UV leakage or under afternoon sunlight of 22 Wm^{-2} UV leakage. The UV leakage was measured by a radiometer from Solar Light Co. PMA 2100 equipped with UV-A, UV-B detectors (260-400 nm) and PAR Quantum Light Sensor (401-700 nm). The coated glass plate was also placed in the cell, but this time without the box, and the coated area faced the lamp by using the same reactor set-up as in the adsorption study.

An aliquot of 0.5 mL of treated phenol was withdrawn from each reactor at a designed time interval for 90 min and was kept in the centrifuge tubes. The concentration of remaining phenol in the solution was analyzed by high-performance liquid chromatography, HPLC (Shimadzu LC-10 ATVP) equipped using a Supelcosil™ LC-18 reversed phase column (250 mm×4.6 mm i.d, with 5 μm particle size) from Sigma Aldrich Co. The eluent was pumped at a rate of 0.5 mL min^{-1} by a binary mixture flow of methanol HPLC grade and ultra-pure water 60/40% (v/v), while the UV detector was operated at 220 nm. The relationship between the peak area and concentration of the remaining phenol was determined using the standards. For reusability test, the TiO_2/PAC plate was used repeatedly and the remaining solution of phenol after one cycle was replaced with the fresh solution before the beginning of the next cycle. Between each cycle, the plate was regenerated using distilled water under the irradiation of the lamp or sunlight. All experiments were done at ambient temperature (30 °C).

6. COD Removal Study

The immobilized TiO_2/PAC and TiO_2 plates used were photoetched prior to eliminate the organic leaching from the degradation of ENR_{50}/PVC binder, which could affect the COD reading [28]. Accurately, 20 mL of 10 mg L^{-1} phenol solution was irradiated for 600 and 180 min using a photocatalytic reactor setup under an indoor fluorescent lamp and solar light, respectively. Another COD removal experiment was done for 60 mg L^{-1} of phenol for a duration of 360 min under solar light irradiation. 2 mL of three portions of treated phenol sample was, respectively, pipetted into three test tubes, each containing 3 mL of COD reagent, by using a micropipette at a designed time interval. The ultra-pure water was used as a blank. All the samples were then refluxed for 120 min using the HACH COD reactor that was pre-heated at 140 °C. The COD concentration was measured using a direct reading spectrophotometer model DR2000 from HACH at 620 nm.

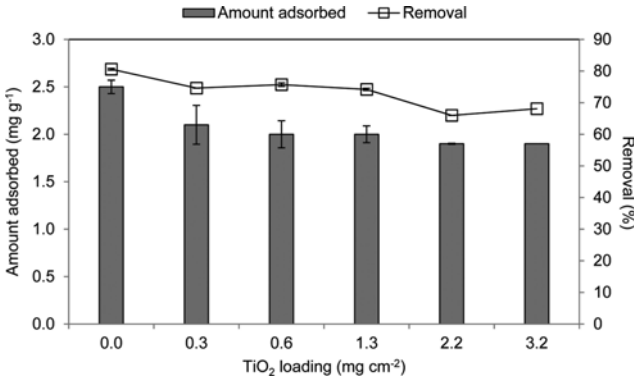

Fig. 1. The amount adsorbed and removal efficiency of phenol by TiO_2/PAC at different TiO_2 loadings [PAC=2.5 mg cm^{-2}; $[Phenol]_o$=10 mg L^{-1}; pH=6; t=90 min; aeration flow rate= 40 mL min^{-1} and T=30 °C].

RESULTS AND DISCUSSION

1. Effect of TiO_2 Loading on Phenol Adsorption

The TiO_2/PAC system was designed to remove phenol via synergistic photocatalytic-adsorptive removal processes. The effect of different TiO_2 loadings on PAC layer in the system on phenol adsorption is presented in Fig. 1, while the respective surface morphology of coated TiO_2 is depicted in Figs. 2(a)-(f). Based on the results presented, adding more TiO_2 on the top of PAC layer caused the amount of phenol adsorbed (q_e) and removal efficiency to decrease from 2.5 to 1.9 mg g^{-1} and 80.6 to 68.1%, respectively. The decrease in both parameters could be explained by the surface morphology of the coated TiO_2 layers as observed at 1,000x and 50,000x of magnifications. From the SEM micrographs, we found that different amount of TiO_2 loaded on PAC gave a significant visual difference in their respective morphology. When 0.3 mg cm^{-2} of TiO_2 was loaded, the cavities on the catalyst surface were clearly visible (Fig. 2(a)) in which the TiO_2 white particles were randomly distributed (Fig. 2(b)). However, when 1.3 mg cm^{-2} of TiO_2 was loaded on the PAC layer, the surface of the photocatalyst layer became compact (Fig. 2(c)) as the pores were partly covered by TiO_2 particles (Fig. 2(d)). The SEM micrograph in Fig. 2(e) reveals that when 2.2 mg cm^{-2} TiO_2 was loaded on the PAC layer, the surface became too compact to the extent that some cracks appeared on the layer surface. The emergence of the cracks was due to the excessive loading of TiO_2 as well as the drying effect of the thick TiO_2 layer during the dip-coating process. The TiO_2 particles covered almost every part of PAC layer, which made the layer become more compact, dense and thicker as seen in Fig. 2(f).

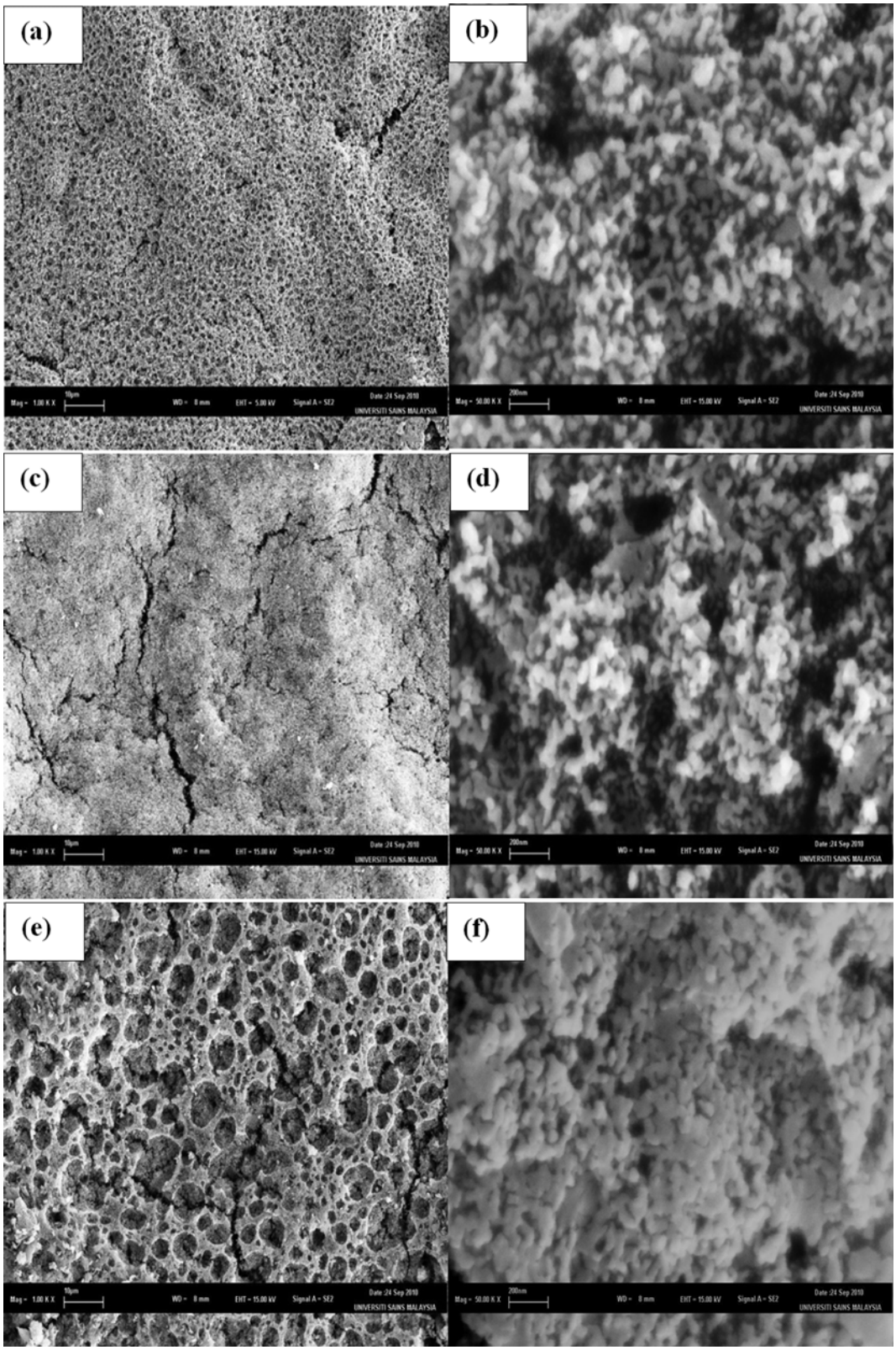

Fig. 2. Surface morphologies of TiO_2 layer on top of PAC layer at (1,000x, 50,000x) magnifications for 0.3 mg cm^{-2} (a), (b) 1.3 mg cm^{-2} (c), (d) and 2.2 mg cm^{-2} (e), (f) of loading.

The BET results shown in Table 1 supported the SEM micrographs on the relation of phenol removal with immobilized TiO_2 loading. A drastic drop in the specific surface area of TiO_2 powder to immobilized TiO_2 occurred with the loading of 0.3 mg cm^{-2}

Table 1. BET results and point of zero charge (pH_{pzc}) for TiO_2 powder and immobilized TiO_2 loadings

Type of TiO_2	Surface area ($m^2\ g^{-1}$)	Pore volume ($\times10^{-1}\ cm^3\ g^{-1}$)	Average pore diameter (nm)	pH_{pzc}
Powder[a]	56	1.78	0.97	4.8
Immobilized (0.3 mg cm^{-2})	19	1.14	23.6	4.4[a]
Immobilized (2.2 mg cm^{-2})	13	0.65	20.5	-

[a]From ref. [28]

from 56 to 19 $m^2\ g^{-1}$. The surface area was reduced further to 13 $m^2\ g^{-1}$ when the loading was 2.2 mg cm^{-2}. The pore volume also decreased from 0.178 to 0.065 $cm^3\ g^{-1}$ while the contrasting result was observed for the pore diameter, which increased drastically when in immobilized form but decreased at higher TiO_2 loading. From the BET perspective, the adsorption of phenol into PAC sublayer was greatly affected by the surface area and pore volume of the TiO_2 top layer. A larger amount of phenol molecules was adsorbed into the PAC layer through the thinner TiO_2 layer due to the bigger surface area and pore volume, while only fewer molecules could penetrate through the thicker TiO_2 due to a limited surface area and pore blockage by the compact layer. Xing et al. [30] also observed that the TiO_2/AC composites with low TiO_2 loading adsorbed dye faster than the composites with high TiO_2 loading due to their larger surface area and pore volume. From these results, we can see that the PAC layer is highly superior to the TiO_2 layer in adsorbing phenol molecules and therefore, only a thin TiO_2 layer was needed in this TiO_2/PAC system.

2. Adsorption Equilibrium

The Langmuir, Freundlich and Temkin isotherm models were used to describe the adsorption process of phenol at equilibrium. Langmuir is valid for monolayer and homogeneous adsorption onto a surface with a finite number identical site. On the other hand, the Freundlich model is an empirical equation based on multilayer sorption on the heterogeneous surface, whereas the Temkin assumes that the heat of adsorption would decrease linearly with coverage [7,31]. The respective non-linear isotherm equations can be seen in Table 2. Here, q_m is the maximum adsorption capacity as calculated by the Langmuir equation (mg g^{-1}), K_L is the Langmuir constant (L mg^{-1}), K_F is the Freundlich constant (L g^{-1}), n is the adsorption intensity (unitless), R is the universal gas constant (8.314 J $mol^{-1}\ K^{-1}$), T is the absolute temperature (K), b_T is the Temkin constant (J mol^{-1}) and A_T is the Temkin equilibrium binding constant (L g^{-1}).

Table 2. Non-linear equation, parameters and error analysis for isotherm models

Model	Equation	Parameters	Error analysis
Langmuir	$q_e = q_m \frac{K_L C_e}{1+K_L C_e}$	q_m=27.8 mg g^{-1}	R^2=0.980
		K_L=0.17 L mg^{-1}	χ^2=0.044
			RMSE=1.02
Freundlich	$q_e = K_F C_e^{1/n}$	1/n=0.516	R^2=0.934
		K_F=4.69 L g^{-1}	χ^2=0.067
			RMSE=1.71
Temkin	$q_e = \ln A_T C_e$	b_T=6.03 J mol^{-1}	R^2=0.717
		A_T=0.015 L mg^{-1}	χ^2=0.147
			RMSE=4.64

The applicability of the isotherm models was compared based on the R^2, χ^2 and RMSE values. From the data also listed in Table 2, it is obvious that the TiO_2/PAC system best-fits the Langmuir model due to the highest R^2 value and lowest error analysis as compared to the Freundlich and Temkin models. The maximum capacity (q_m) as determined by TiO_2/PAC was found to be 27.8 mg g^{-1}. The presence of TiO_2 top layer on the PAC layer induced a homogeneous and monolayer adsorption. All the adsorption sites are finite with each adsorbate molecule adsorbed onto the surface has equal sorption activation energy [32]. According to Heraldy et al., monolayer adsorption is formed when the bonding strength of adsorbate and the adsorbent surface is stronger than the adsorbate-adsorbate, adsorbate-solvent, adsorbent-solvent and solvent-solvent bonding. In this case, the first adsorbed phenol will be the initiator molecule in which the adjacent molecule will be tied to it horizontally due to the strong photocatalyst-phenol interaction. They added that the termination of monolayer adsorption would be either by the equilibrium or irreversible mechanism [33]. Another feature that could be deduced from the Langmuir isotherm was the adsorption favorability in terms of the separation factor, R_L, which is defined according to the following Eq. (6): [32]

$$R_L = \frac{1}{(1+K_L C_o)} \quad (6)$$

The R_L value indicates the shape of the isotherm is either to be unfavorable (R_L>1), linear (R_L=1), favorable (0<R_L<1) or irreversible (R_L=0). For all the concentrations studied, the R_L values in Table 3 were in the range of 0<R_L<1, which showed that the adsorption of phenol onto TiO_2/PAC was favorable. Meanwhile, the point of zero charge (pH_{pzc}), which was at 4.4, denoted that the adsorption of phenol favorably occurred on TiO^- surface as the working pH in this study was pH 6 [19].

3. Adsorption Diffusion

To understand the diffusion of phenol into the TiO_2/PAC system, the adsorption data were analyzed from the mechanical point of view using Weber-Morris equation as shown below:

Table 3. R_L values for adsorption of phenol onto TiO_2/PAC at different initial concentrations

Initial concentration (mg L^{-1})	R_L values
10	0.38
20	0.23
30	0.17
60	0.09
100	0.06

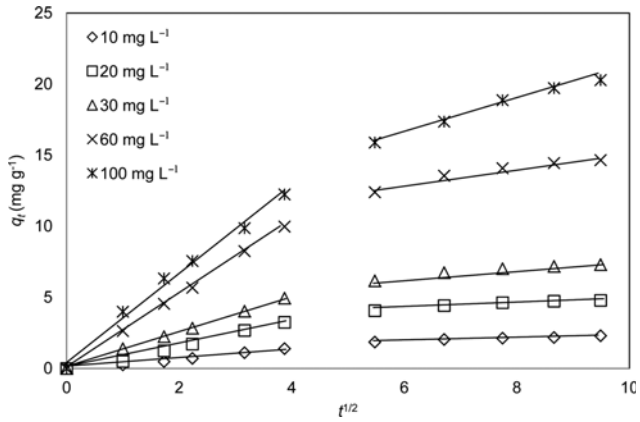

Fig. 3. Intra-particle diffusion for adsorption of phenol onto immobilized TiO_2/PAC at different initial concentrations [TiO_2= 0.3 mg cm^{-2}; PAC=2.5 mg cm^{-2}; pH=6; t=90 min; aeration flow rate=40 mL min^{-1} and T=30 °C].

$$q_t = k_{di} t^{1/2} + C \quad (7)$$

Here, k_{di} (mg g^{-1} $min^{-1/2}$) is the intra-particle diffusion rate constant, i is the stage number and C is the y-intercept corresponding to the degree of boundary layer thickness. Weber and Morris proposed that the adsorbate uptake varies almost proportionally with $t^{1/2}$ rather than the contact time, t, and a plot of q_t versus $t^{1/2}$ should be a straight line with a slope k if intra-particle diffusion is the rate-limiting step [34]. The straight-line plot for the TiO_2/PAC system Fig. 3 shows multi-linearity for every concentration used. The first stage of each concentration produces a linear plot that passes through the origin where the k_{d1} values of the TiO_2/PAC system in Table 4 were derived from the slopes. This first stage was due to the intra-particle diffusion, which is the rate-limiting stage. Apparently, the effect of the boundary layer is not significant since the adsorption process was carried out under turbulent aerated condition. The k_{d1} values increased with increasing concentration, showing that fast adsorption of phenol by the mesoporous structure of TiO_2 top layer into the PAC sub-layer at the first stage. As the mesoporous reached saturation, phenol diffused in the micropores within the two layers [34]. This second stage is attributed to the final equilibrium for which the diffusion started to cease due to extremely low phenol concentration left in solution and an increase in the diffusion resistance, which slowed the diffusion rate as shown by the low k_{d2} values. The same phenomenon was also observed when using immobilized montmorillonite for the methylene blue uptake [34].

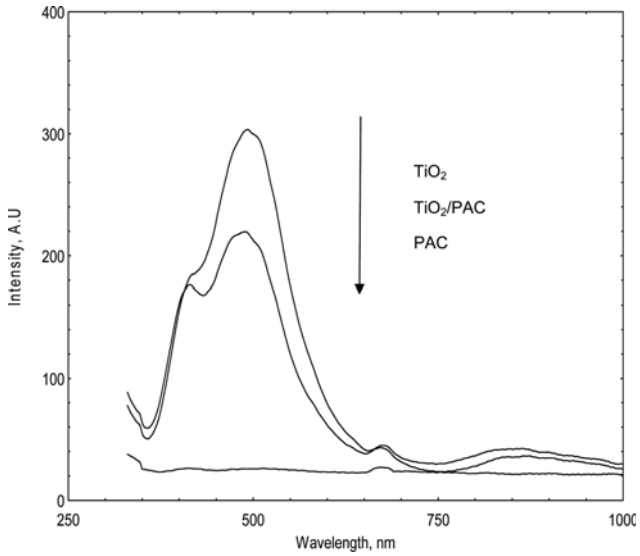

Fig. 4. Photoluminescence spectra of different immobilized systems in TiO_2/PAC.

Table 4. Intra-particle diffusion parameters at different concentrations of phenol

$[Phenol]_o$ (mg L^{-1})	K_{d1} (mg g^{-1} $min^{-1/2}$)	R^2	K_{d2} (mg g^{-1} $min^{-1/2}$)	R^2
10	0.369	0.987	0.103	0.974
20	0.877	0.988	0.179	0.937
30	1.26	0.999	0.277	0.943
60	2.57	0.999	0.553	0.940
100	3.32	0.991	1.23	0.986

4. Adsorption Thermodynamics

The operation temperature can affect the phenol adsorption onto the TiO_2/PAC; thus a thermodynamic study was carried out within the temperature range of 30-60 °C. The changes in Gibbs free energy (ΔG^o), enthalpy (ΔH^o) and entropy (ΔS^o) were evaluated using the corresponding thermodynamic equations [35]:

$$K_C = \frac{C_{Ae}}{C_e} \quad (8)$$

$$\Delta G^o = -RT \log K_C \quad (9)$$

$$\log K_C = \frac{\Delta S^o}{2.303R} - \frac{\Delta H^o}{2.303RT} \quad (10)$$

where K_C is the equilibrium constant, C_{Ae} is the concentration of phenol adsorbed on TiO_2/PAC at equilibrium (mg L^{-1}) and C_e is the concentration of phenol remained in the solution (mg L^{-1}) at equilibrium. A graph of log K_C versus 1/T was plotted where the values of ΔH^o and ΔS^o were calculated from the slope and intercept, respectively.

Table 5 shows the calculated thermodynamic parameters at different reaction temperature for phenol uptake onto the TiO_2/PAC. The negative and increasing ΔG^o values with temperature show that the process of phenol uptake onto the TiO_2/PAC system occurred spontaneously, but became increasingly unfavorable at a

Table 5. Thermodynamic parameters at different reaction temperatures

Temperature (K)	ΔG^o (kJ mol^{-1})	ΔH^o (kJ mol^{-1})	ΔS^o (kJ mol^{-1} K^{-1})	R^2
300	−3.12	98.2	36.6	0.988
318	−2.08			
333	−1.56			

higher temperature. This also means that the immobilized system could reduce the operation cost as it works better at room temperature. Meanwhile, the positive values exhibited by ΔH^o and ΔS^o denoted an endothermic adsorption process and an increase in the randomness of phenol and immobilized TiO_2/PAC for which the displacement of water molecules by phenol was observed [36].

5. PL Analysis

Photoluminescence (PL) analysis can investigate the optical and surface properties of immobilized TiO_2, TiO_2/PAC and PAC. The analysis was done prior to observing the effect of combining TiO_2 and PAC as TiO_2/PAC layer by layer as opposed to the monolayer systems, respectively. The PL spectrum in Fig. 4 shows that the peak intensity of TiO_2 monolayer is the highest as compared to the TiO_2/PAC and PAC monolayer. This high degree of intensity was related to the high PL emission that was emitted from the high recombination rate of electron-hole (e^--h^+) pairs during the transition of the electron from the valence band to the conduction band of TiO_2. The energy that was released from the radiation of photon corresponded to PL emission and band gap energy.

According to Liqiang et al. [37], there are two possible explanations for the relation of PL emission intensity and photocatalytic activity. For the first reason, the PL peak at 420 nm is coming from

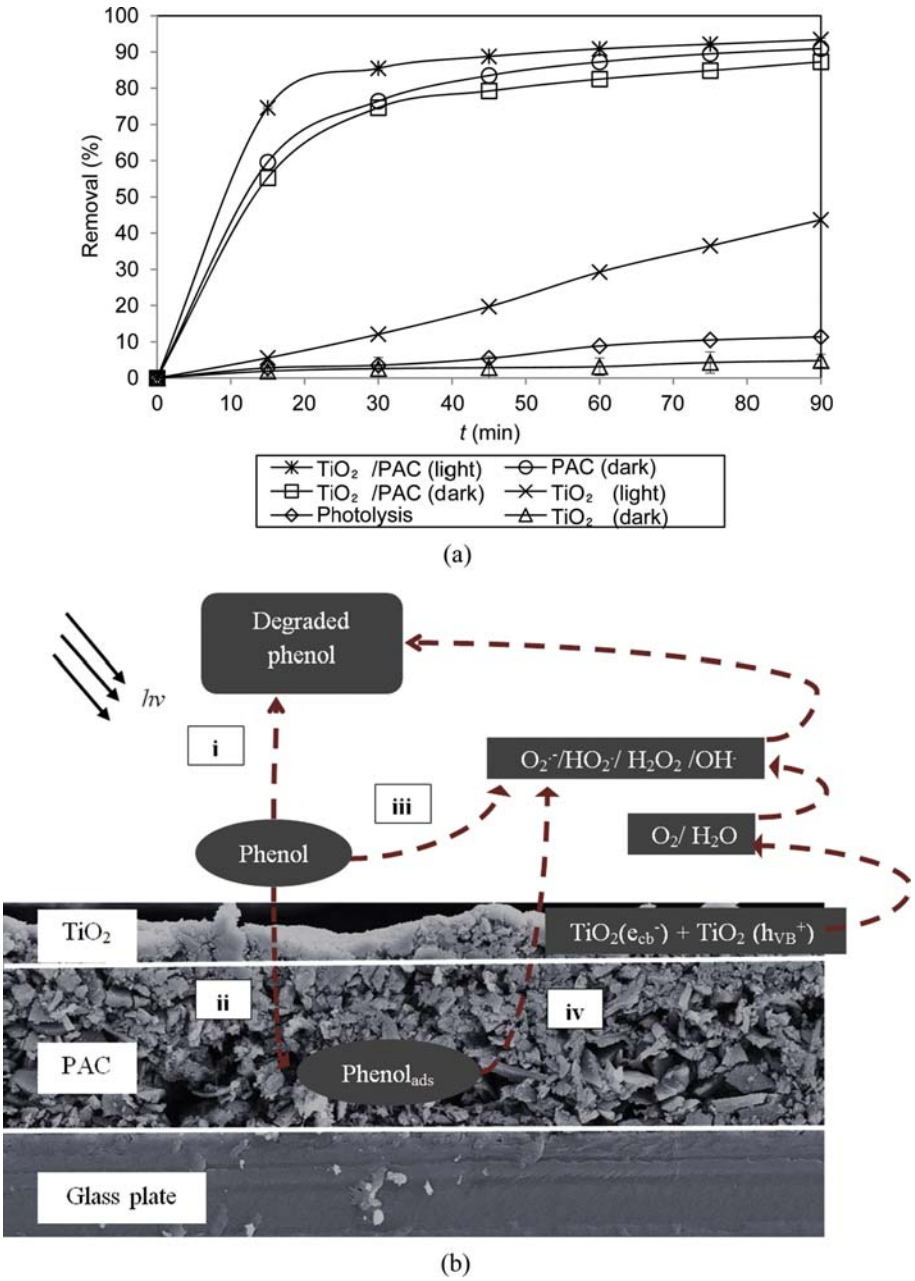

Fig. 5. (a) Comparison on the removal efficiency of phenol by photolysis, TiO_2/PAC and TiO_2 under indoor lamp and in the dark, and PAC in the dark; (b) schematic diagram of photocatalytic-adsorptive removal mechanism by TiO_2/PAC layer by layer under light irradiation as modified from reference [39].

band edge free excitons, while the peak at 480 nm is attributed to excitonic PL process. The higher the PL peak intensity at both wavelengths is, the higher is the surface oxygen vacancy and defect. This type of PL peak is said to happen to the semiconductor with dopant species. On the other hand, the second reason is that if the PL peak is lower, the recombination of e^--h^+ pairs is lesser. As a result, the photocatalytic reaction becomes more effective. Apparently, for this TiO_2/PAC system case, the second explanation relates well since the presence of PAC functions as the adsorbent sub-layer, not as a dopant for TiO_2. In addition, PAC can capture electron during the e^--h^+ generated TiO_2 as proven by the lower PL peak showed by TiO_2/PAC system. However, for PAC, there was no PL emission detected, showing that the electron was not prone to excitation. Therefore, in TiO_2/PAC system, the lower PL intensity than TiO_2 monolayer was related to the lower recombination of charge carriers on the TiO_2 surface, which was attributed from the presence of PAC that increased the lifetime of charge carrier and consequently would improve the photocatalytic activity.

6. Photocatalytic-adsorptive Removal Efficiency by TiO_2/PAC and its Mechanism

It is generally accepted that the TiO_2 top layer plays the main role in the photocatalytic oxidation of pollutants, while the PAC sub-layer accumulates the adsorbed phenol [38]. However, the process performance by the individual and combined system needs to be compared to see the relative contribution from each process and identify their synergism for phenol removal by the TiO_2/PAC system. Fig. 5(a) shows the percentage of phenol removed after 90 min of individual treatment by photolysis, TiO_2/PAC by photocatalytic-adsorptive removal, TiO_2/PAC, TiO_2 and PAC by adsorption and TiO_2 by photocatalysis. Photolysis by itself could remove 11.4% of phenol, while phenol adsorption by PAC monolayer in the dark removed 87.3% of the pollutant. On the other hand, TiO_2 monolayer only oxidized 43.7% of phenol, while TiO_2/PAC by photocatalytic-adsorptive removal degraded 93.4% of phenol. The poor photoactivity of TiO_2 was due to the poor adsorption of the photocatalyst which could only remove 4.8% of phenol. An improvement in the removal efficiency was observed for the TiO_2/PAC system upon irradiation due to the synergistic effect of photocatalysis by the TiO_2 top layer and adsorption by the PAC sub-layer. The PAC layer accumulated the phenol molecules, concentrated and brought them to a close contact with TiO_2 active sites, while the TiO_2 layer oxidized the adsorbed phenol. More phenol was removed from the solution in the presence of PAC sub-layer, which proved again that the adsorption by PAC layer plays the key role in the total removal of phenol in TiO_2/PAC system. These observations also confirmed that the adsorbent plays a crucial role in improving the photocatalytic reaction on the TiO_2's surface since TiO_2 has poor adsorption capacity towards some organic pollutants [9].

To understand the phenol removal by TiO_2/PAC, the following mechanism is proposed. As illustrated in the cross-section of TiO_2/PAC in Fig. 5(b), there are five pathways for removing phenol. Upon light irradiation, some phenols were directly removed by photolysis **(i)**. However, most of them would pass through the TiO_2 layer and accumulate in the PAC layer **(ii)**. At the same time, the electrons at the valence band of TiO_2 were excited under light irradiation and produced photo-generated holes (h_{VB}^+) and electrons (e_{CB}^-) at the valence and conduction band of TiO_2, respectively, which later reacted with H_2O and O_2 to become active radicals ($O_2^{\cdot-}$/$HO_2^{\cdot}$/$OH^{\cdot}$/H_2O_2). Direct photocatalytic oxidation of phenol occurred at the TiO_2 surface **(iii)**. The radicals would diffuse to the interface of TiO_2/PAC due to the mesoporous structure within TiO_2 layer and oxidize the accumulated phenol in PAC sub-layer (route not shown) [39]. Other adsorbed phenols were forced to pass through the TiO_2 layer again due to concentration gradient effect by the remaining phenol solution where they would be also oxidized by the active radicals within or at the surface of the TiO_2 layer, formed intermediates and eventually mineralized to CO_2 and H_2O **(iv)**. The homogeneous distribution of phenol within the TiO_2/PAC would result in a complete photocatalytic-adsorptive removal [40].

7. Reusability

One of the advantages of the immobilized system is it can be reused for continuous cycles in practical and large-scale applications. This is important for the wastewater treatment operations to save energy, cost and material, besides effectively removing the pollutants. We used four different experimental conditions that involved reusability at 10 and 60 mg L^{-1} concentrations of phenol and each under the irradiation of the 45-W fluorescent indoor lamp and solar light.

Fig. 6 shows the comparison of synergistic photocatalytic-adsorptive removal by TiO_2/PAC after 90 min at different concentrations (10 mg L^{-1} and 60 mg L^{-1}) and light sources (lamp and solar) for ten cycles. Under the solar light, 97.3±0.5% of 10 mg L^{-1} phenol was removed from the solution, while the removal was 91.3±2.1% for 60 mg L^{-1} of phenol at the first cycle. Meanwhile, for the experiment under lamp irradiation, the removal was 93.4±0.4% using 10 mg L^{-1} of phenol, whereas, it was 88.8±1.3% for 60 mg L^{-1} of phenol at the first cycle. On the average, 97.7±0.9% of 10 mg L^{-1} phenol was removed under solar irradiation throughout 10 cycles, while it was 89.1±2.5% for 60 mg L^{-1} phenol. Under lamp irradiation, the average removal was 86.4±2.1% and 67.9±7.6% for 10 mg L^{-1} and 60 mg L^{-1} of phenol, respectively. The photocatalytic-adsorptive removal process of phenol was faster at low concentration (10 mg L^{-1}) and under solar light irradiation than high concentration (60 mg L^{-1}) and under the indoor lamp. The phenol re-

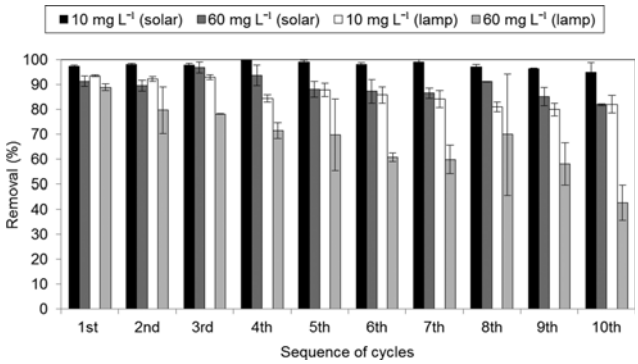

Fig. 6. Reusability of TiO_2/PAC by means of removal efficiency after 90 min for different phenol concentrations and light sources [TiO_2=0.3 mg cm^{-2}; PAC=2.5 mg cm^{-2}; pH=6; t=90 min; aeration flow rate=40 mL min^{-1} and T=30 °C].

moval efficiency slightly decreased after each reuse for all the conditions, especially for 60 mg L^{-1} of phenol, because most of the pores had been filled up with phenols. This is understandable because each reuse of the same plate would use up some of the adsorption active sites of the PAC sub-layer. Therefore, the contribution from the adsorption process would tend to decrease with each reuse cycle. Apparently, the phenol removal efficiency by TiO_2/PAC under solar light seemed to be sustainable as the efficiency of the first cycle for both concentrations was very close to the average value, thus giving the constant photocatalytic-adsorptive removal throughout the ten cycles. This is because solar light contains high photon energy which can surpass the band gap energy of TiO_2. This phenomenon could initiate the charge separation of electron and hole in TiO_2 more effectively and promote rapid photocatalytic oxidation of the adsorbed phenol [27].

8. COD Removal

The photocatalytic oxidation of phenol initiates the opening of aromatic chain to the aliphatic chain via the $^{\bullet}OH$ radicals attack before fully converts them into CO_2 and H_2O as shown by the following equation:

$$C_6H_5OH+7O_2 \xrightarrow{TiO_2/PAC,\ H_2O,\ h\nu} \text{Intermediates} \xrightarrow{^{\bullet}OH} 6CO_2+3H_2O \quad (11)$$

Chemical oxygen demand (COD) is an indicator in photocatalysis which functions as a general measurement for the amount of carbonaceous substances present in the treated solution, which is reported as COD values [10,41]. For a typical COD determination, a strong oxidant, $K_2Cr_2O_7$ was preferable while $AgSO_4$ used with COD reagent acted as the catalyst to achieve complete oxidation of pollutants [42,43]. Some amount of $HgSO_4$ was also added to the COD reagent in order to remove possible Cl^- ions interference [44]. The COD removal experiment was done under an indoor lamp and solar light irradiation using phenol solutions with concentrations of 10 mg L^{-1} (lamp and solar light) and 60 mg L^{-1} (solar light), and was compared against TiO_2 monolayer.

The plates were photoetched before the experiment to eliminate the interfering leached organic substance from TiO_2 layer taking place upon irradiation. The initial COD value of 10 mg L^{-1} phenol was 30±2 mg L^{-1}, while it was 138±5 mg L^{-1} for 60 mg L^{-1}. As seen in Fig. 7, the COD values decreased for all conditions, reflecting an increase in the amount of organic carbon oxidized to CO_2 with irradiation time. Apparently, a complete COD removal of 10 mg L^{-1} phenol by TiO_2/PAC was achieved within 600 min for the experiment under lamp irradiation. On the other hand, under solar light, the COD removal by TiO_2/PAC needed only 180 min of irradiation time for the same concentration, while it required more than 600 min to reduce the COD concentration of 60 mg L^{-1} of phenol. Meanwhile, the TiO_2 monolayer took more than 600 min to oxidize 10 mg L^{-1} of phenol under the indoor lamp and showed slower trend than TiO_2/PAC in the COD removal of 60 mg L^{-1} phenol under solar light. It was evidenced that under solar irradiation and at 10 mg L^{-1} phenol, the COD removal by TiO_2/PAC was faster than indoor lamp since the high energy provided by sunlight favored the TiO_2 photocatalytic oxidation. On the other hand, at high concentration, more phenols were present that would compete for active radicals and thus slowed down the photocatalytic oxidation process. The slow COD removal trend as shown by TiO_2 monolayer under the indoor lamp and solar light proved that the PAC sub-layer predominantly aided in the removal process by bringing phenol closer to TiO_2 active sites for photocatalytic oxidation occurrence. The positive impact of synergism of TiO_2/PAC combination was also observed for COD removal of phenol derivatives using TiO_2/AC fiber [45] and TiO_2/PAC mixture [46].

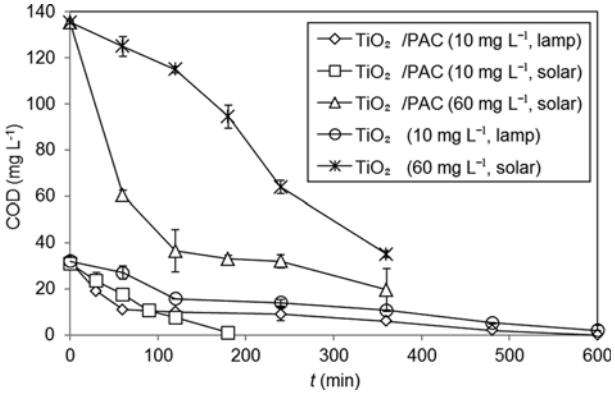

Fig. 7. COD values as a function of irradiation time for photocatalytic oxidation of 10 and 60 mg L^{-1} phenol by TiO_2/PAC and TiO_2 monolayer under different light sources [TiO_2=0.3 mg cm^{-2}; PAC=2.5 mg cm^{-2}; pH=6; t=90 min; aeration flow rate= 40 mL min^{-1} and T=30 °C].

CONCLUSION

This batch study presents a new way of combining TiO_2 and PAC for the wastewater treatment plant and solar application. The loading of TiO_2 on PAC sub-layer layer influenced the amount of phenol adsorbed, and its removal efficiency with thinner layer had higher surface area and would allow better diffusion of phenol into PAC layer than the thicker TiO_2 top layer. Phenol adsorption onto TiO_2/PAC obeyed the Langmuir isotherm model, which exhibited a monolayer and homogeneous adsorption. The rate-limiting step of adsorption by TiO_2/PAC was controlled by intra-particle diffusion, while the thermodynamic study showed spontaneous and endothermic nature of adsorption. The inclusion of PAC as a sub-layer of TiO_2 reduced the PL emission, which indicated effective charge separation. The combination of TiO_2/PAC via layer by layer assemblage improved the removal efficiency of phenol by two-fold than the TiO_2 monolayer. The reusability of TiO_2/PAC was quite sustainable under UV-vis and total visible irradiation, which the latter shows the possibility of a real application. Fast COD removal by TiO_2/PAC occurred at a low concentration of phenol and under solar light irradiation as fewer phenol molecules and high photon energy favor photocatalytic oxidation. It was evidenced that the TiO_2/PAC is a better system than TiO_2 monolayer based on the phenol and COD removal due to the synergy processes from adsorption by the PAC sub-layer and photocatalysis by the TiO_2 top layer.

ACKNOWLEDGEMENTS

The authors would like to thank Universiti Sains Malaysia (USM)

for the research and financial support through USM-PRGS Grant No. 1001/PKIMIA/843034. N.N. Bahrudin was grateful to USM for the graduate assistantship (GA) and Malaysian Ministry of Higher Education for financial assistance under the Budget Mini Programme.

REFERENCES

1. P. Saravanan, K. Pakshirajan and P. Saha, *J. Hydro-environ. Res.*, **3**, 45 (2009).
2. V. Duma, K. Popp, M. Kung, H. Zhou, S. Nguyen, S. Ohyama, H. Kung and C. Marshall, *Chem. Eng. J.*, **99**, 227 (2004).
3. Z. Guo, R. Ma and G. Li, *Chem. Eng. J.*, **119**, 55 (2006).
4. I. Fierascu, S. M. Avramescu, I. Petreanu, A. Marinoiu, A. Soare, A. Nica and R. C. Fierascu, *React. Kinet. Mech. Cat.*, **122**, 155 (2017).
5. P. Girods, A. Dufour, V. Fierro, Y. Rogaume, C. Rogaume, A. Zoulalian and A. Celzard, *J. Hazard. Mater.*, **166**, 491 (2009).
6. H. Mahadevan, V. V. Dev, K. A. Krishnan, A. Abraham and O. Ershana, *Environ. Technol. Innovation*, **9**, 1 (2018).
7. P. Baldrick, *Regul. Toxicol. Pharm.*, **56**, 290 (2010).
8. S. Saran, G. Manjari, P. Arunkumar and S. P. Devipriya, *Korean J. Chem. Eng.*, **34**, 2984 (2017).
9. H. Dong, G. Zeng, L. Tang, C. Fan, C. Zhang, X. He and Y. He, *Water Res.*, **79**, 128 (2015).
10. M. Farzadkia, Y. Dadban Shahamat, S. Nasseri, A. H. Mahvi, M. Gholami and A. Shahryari, *J. Eng.*, **2014**, 10 (2014).
11. D. Dubber and N. F. Gray, *J. Environ. Sci. Health, Part A*, **45**, 1595 (2010).
12. H. A. Rangkooy, M. N. Pour and B. F. Dehaghi, *Korean J. Chem. Eng.*, **34**(12), 3142 (2017).
13. R. R. Kalantary, Y. Dadban Shahamat, M. Farzadkia, A. Esrafili and H. Asgharnia, *Desalin. Water Treat.*, **55**, 555 (2015).
14. P. N. Omo-Okoro, A. P. Daso and J. O. Okonkwo, *Environ. Technol. Innovation*, **9**, 100 (2018).
15. C. Sriwong, S. Wongnawa and O. Patarapaiboolchai, *J. Environ. Sci.*, **24**, 464 (2012).
16. C. Andriantsiferana, E. F. Mohamed and H. Delmas, *Environ. Technol.*, **35**, 355 (2014).
17. B. Xing, C. Shi, C. Zhang, G. Yi, L. Chen, H. Guo, G. Huang and J. Cao, *J. Nanomater*, **2016**, 10 (2016).
18. A. C. Martins, A. L. Cazetta, O. Pezoti, J. R. B. Souza, T. Zhang, E. J. Pilau, T. Asefa and V. C. Almeida, *Ceram. Int.*, **43**, 4411 (2017).
19. Y. S. Ngoh and M. A. Nawi, *Mater. Res. Bull.*, **76**, 8 (2016).
20. A. H. Jawad and M. A. Nawi, *React. Kinet. Mech. Cat.*, **106**, 49 (2012).
21. J. Shi, J. Zheng, P. Wu and X. Ji, *Catal. Commun.*, **9**, 1846 (2008).
22. G. L. Puma, A. Bono, D. Krishnaiah and J. G. Collin, *J. Hazard. Mater.*, **157**, 209 (2008).
23. L. Andronic and A. Duta, *Thin Solid Films*, **515**, 6294 (2007).
24. A. López, D. Acosta, A. I. Martínez and J. Santiago, *Powder Technol.*, **202**, 111 (2010).
25. B. Stefanov and L. Österlund, *Coatings*, **4**, 587 (2014).
26. M. Zafar, J.-Y. Yun and D.-H. Kim, *Korean J. Chem. Eng.*, **35**, 567 (2017).
27. N. N. Bahrudin and M. A. Nawi, *React. Kinet. Mech. Cat.*, **124**, 153 (2018).
28. M. A. Nawi and S. M. Zain, *Appl. Surf. Sci.*, **258**, 6148 (2012).
29. F. Marrakchi, W. Khanday, M. Asif and B. Hameed, *Int. J. Biol. Macromol.*, **93**, 1231 (2016).
30. B. Xing, C. Shi, C. Zhang, G. Yi, L. Chen, H. Guo, G. Huang and J. Cao, *J. Nanomater*, **2016**, 3 (2016).
31. A. Dada, A. Olalekan, A. Olatunya and O. Dada, *IOSR J. Appl. Chem.*, **3**, 38 (2012).
32. S. Nethaji, A. Sivasamy and A. Mandal, *Int. J. Environ. Sci. Technol.*, **10**, 231 (2013).
33. E. Heraldy, Y. Hidayat and M. Firdaus, *IOP Conf. Series: Mater. Sci. Eng.*, **107**, 012067 (2016).
34. Y. S. Ngoh and M. A. Nawi, *Int. J. Environ. Sci. Technol.*, **13**, 907 (2016).
35. M. A. Nawi, S. Sabar, A. H. Jawad, Sheilatina and W. S. W. Ngah, *Biochem. Eng. J.*, **49**, 317 (2010).
36. R. Ansari, Mohammad-khah and M. Nazmi, *Current Chem. Lett.*, **2**, 215 (2013).
37. J. Liqiang, Q. Yichun, W. Baiqi, L. Shudan, J. Baojiang, Y. Libin, F. Wei, F. Honggang and S. Jiazhong, *Sol. Energy Mater. Sol. Cells*, **90**, 1773 (2006).
38. S. Sabar and M. A. Nawi, *Desalin. Water Treat.*, **57**, 10312 (2016).
39. M. A. Nawi, S. Sabar and Sheilatina, *J. Colloid Interface Sci.*, **372**, 80 (2012).
40. T. Ghosh and W.-C. Oh, *Asian J. Chem.*, **24**, 5419 (2012).
41. Y. D. Shahamat, M. Farzadkia, S. Nasseri, A. H. Mahvi, M. Gholami and A. Esrafili, *J. Environ. Health Sci. Eng.*, **12**, 50 (2014).
42. J. Chen, J. Zhang, Y. Xian, X. Ying, M. Liu and L. Jin, *Water Res.*, **39**, 1340 (2005).
43. Y. W. Kang, M.-J. Cho and K.-Y. Hwang, *Water Res.*, **33**, 1247 (1999).
44. M. Kolb, M. Bahadir and B. Teichgräber, *Water Res.*, **122**, 645 (2017).
45. P. Jin, R. Chang, D. Liu, K. Zhao, L. Zhang and Y. Ouyang, *J. Environ. Chem. Eng.*, **2**, 1040 (2014).
46. K. Baransi, Y. Dubowski and I. Sabbah, *Water Res.*, **46**, 789 (2012).